Cylinder Detection From RGBD Data Based on Radius Estimation Using Number of Measurement Points

Tomoki Kawagoshi[1] and Kimitoshi Yamazaki[1]

Abstract— **In this paper, we describe a method to estimate cylindrical parameters using RGBD data. As cylindrical shape is one of the shape elements that composes of a building, to know cylindrical parameters accurately is useful to robots aiming to grasp such part. Therefore, we propose a method to estimate the diameter and the inclination of a cylinder part. We formulate the relationship between cylinder diameter and the number of 3D points measured from the cylinder. It enables to estimate cylinder diameter from measured point cloud directly. Through proof experiments, we show that our method is more accurate than conventional methods. Moreover, as an example of the search activity at disaster environments, we report an experiment on grasping a ladder by an autonomous mobile manipulator and showed the effectiveness of the proposed method.**

I. Introduction

Cylindrical shape is one of the shape elements that composes of a building. For example, in public facilities and manufacturing plants, cylindrical shapes are used for various parts such as handrails of stairs, door handles, and ladders. One of the roles of such parts is to provide users with a gripping position. It enables to support walking as a handrail, and enables easily to open and close a door as a handle.

Our group is engaged in studies on disaster response robots. In particular, for the purpose of collecting information and searching in the disaster affected buildings, we have coped with remote control robots [1]. Such robots can be of various types such as wheel type and snake type. Among them, it is effective to use a robot with human-like limbs when focusing on mobility and workability [2]. In order for such robots to move in various places, it is considered that various interactions with the surrounding environment are required, e.g. grasping a handrail to prevent a fall or climbing a ladder. For instance, large-scale facilities such as power plants, handrails, handles and ladders are often cylindrical components. Therefore if it is possible to accurately recognize and grasp such cylindrical parts, it can contribute to the improvement of mobility.

The purpose of this study is to obtain cylindrical parameters such as the thickness. This result is used to accurate grasping of cylinder part inside the building by remote control robots as explained the above. Of course, we already have good choices that are implementations of cylinder model fitting, e.g. functions in Point Cloud Library(PCL) [3]. However, as introduced in the experimental section, we often experienced that an error of 5mm or more occurred in the diameter estimation by such a function. On the other hand, for example, when a life-sized robot remotely-controlled goes up and down a ladder, it is extremely important to accurately recognize the thickness and position of a cylinder part when putting a hand on it. Even when using positioning techniques relying on proximity sensors on the palm, we had an impression that the allowable error is less than 5 mm. Therefore, it is required to improve the accuracy of diameter estimation more than the conventional methods.

In this paper, we propose a method for cylinder diameter estimation using 3D range image sensor. The contributions are as follows:

- We propose a novel method for accurately estimating the diameter of a cylinder from the relationship between the measured area of the cylinder and the number of measurement points. We formulate the relationship, and then verified it using actual measurement data obtained from a commonly used 3D range image sensor.
- We confirmed that the above method reduces the estimation accuracy when measuring a thin cylinder from a distance. Therefore, we propose a method to suppress the decrease in accuracy by combining the results of edge detection extracted from color images.
- As an example of the search activity at disaster environments, we conducted an experiment on grasping a ladder by a remote controll robot and showed the effectiveness of the proposed method.

This paper is organized as follows. In the next section we introduce related work. The third section explains our problem setting and approach. The fourth section explains a method to estimate the diameter of cylinder from pairs of depth image and color image. The fifth section describes some proof experiments and discussion. The sixth section concludes this paper.

II. Related work

Cylinder is one fundamental primitive that forms object shape. Therefore it has been a target of shape primitive detection as the same as edges and planes. After range sensors such as laser scanners and 3D range image sensors are actively commerced, many methods for shape primitive detection have been proposed in the fields of computer graphics and robotics.

Schnabel et al. [4] proposed a detection method for several types of shape primitives including cylinders. They used RANSAC [5], which is one practical method for robust estimation. Besides that, RANSAC-based methods for shape

[1]Tomoki Kawagoshi and Kimitoshi Yamazaki are with AIS Lab., Faculty of Engineering, Shinshu University, 410, Mech. Sys. Eng. Buidling, 4-17-1, Wakasato, Nagano, Nagano, Japan {kyamazaki}@shinshu-u.ac.jp

primitive detection is implemented in PCL [3], and it is widely used [6][7]. Also, Vosselman et al. [8] proposed a two-step procedure for Hough transform based detection of cylinders that uses estimated normals in the data points. Recently Harada et al. [10] and Figueiredo et al. [11] proposed methods to detect cylinders from point clouds obtained by measuring a cluttered table.

Forest investigation is another application on cylinder shape detection. Lalonde et al. [12] proposed a method of tree trunk detection from 3D point clouds. In the method, a point cloud that measured many trunks and leaves is input, and then a two stage processing consisting of candidates detection and posture registration is applied. Horiuchi [13] aims to estimate the amount of biomass, and proposed a method to estimate diameter of tree trunk after extracting trunk candidates from a point cloud.

Almost above-mentioned studies took point cloud as input and emphasized to extract shape primitives regarded as a cylinder. That is, the important thing is to seek point cloud well-matching with cylinder shape from clutter scene. On the other hand, as far as the authors know, methods to accurately measure the cylindrical shape of originally cylindrical object have not deeply been studied. Rabbani et al.[9] proposed a cylindrical shape detection based on Hough transformation, then proved the effectiveness of the method by finding pipes in plants. However, their report lacks detail descriptions about the accuracy of detection results such as the error of cylinder diameter. Meanwhile, Figureiredo et al. [11] and Trung et al. [14] evaluated the results of cylinder shape estimation quantitatively, and they describe that about 20mm error remains by their method. Besides they mentioned that the accuracy is almost the same as the result by the method proposed by Rabbani et al.

The motivation of this study is already described in the first section: we propose a novel method to find cylinder diameter because the important thing is to estimate cylindrical shapes more accurate than previous work. We assume that cylindrical parts exist in somewhat sparse environments (like a ladder bars) and operators roughly indicate a spatial position where a cylindrical part exists.

III. Approach

Assuming that a mobile robot mounting a 3D range image sensor is moved by tele-operation. The sensor provides a pair of color image and depth image. In the proposed method, cylinder diameter is estimated from each of the images, and then a final result is obtained by combining the two results.

Figure 1 shows the overall procedure of the proposed method. Cylinder diameter is firstly estimated using a depth image. Based on the result, another diameter estimation is performed using a color image. These processes are adopted to several frames, and finally they are probabilistically combined.

As a first step in the processing of a depth image, we define a spherical region centering a point on the surface of a cylinder. This point can be both manually defined and automatically detected. Next, we convert a depth image to

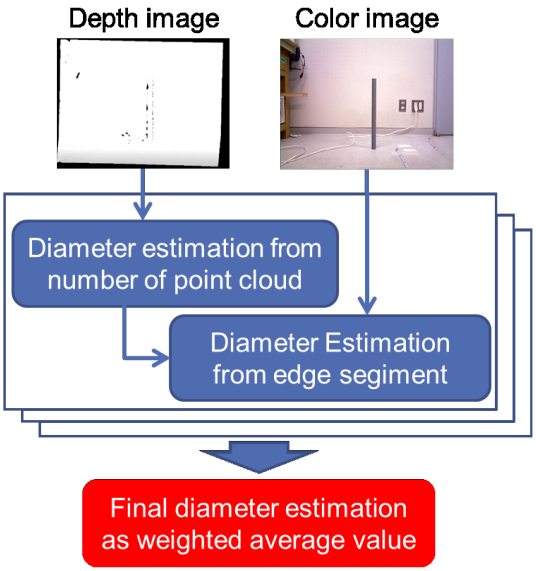

Fig. 1. Overall procedure of the proposed method

3D point cloud. Counting the number of points within the spherical region and measuring the distance between the sensor and the cylinder surface, we then calculate a diameter value based on the relationship of the two results mentioned the above. One advantage of the method of counting the number of points is robustness to poor repeatability of distance measurement. For instance, there are methods to estimate cylinder parameters using normal information. Such methods require to calculate a normal vector per point by making local plane from neighboring points. This process easily becomes unstable when distance measurement is poor repeatability. Comparing with them, the method counting the number of points is simple but robust.

Meanwhile, in the processing of a color image, we first detect image edges, then select candidate edges of the contour of cylinder from them. In this process, the estimation result by depth images is partly used. Then, we estimate a cylinder diameter based on the distance of the two opposite edges. We repeat the above processes several times, and calculate the average and variance of diameter value. Based on the reliability value calculated from them, we obtain the final estimation result.

In the procedure mentioned the above, color image processing depends on the result of depth image processing. Therefore, the two processes do not independent. However, as described later, we can logically show that the error on the depth image processing does not significantly affect the color image processing. Therefore it is considered that the proposed procedure is equivalent to the following process: Two diameter values are calculated from a depth image and a color image, respectively, and then these values are used to generate a unified result.

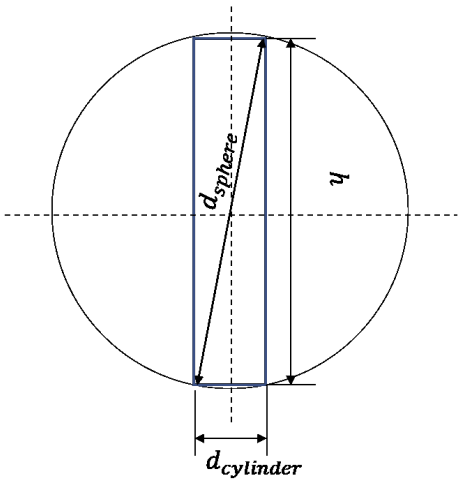

Fig. 2. A relationship between the cylinder part and the spherical region

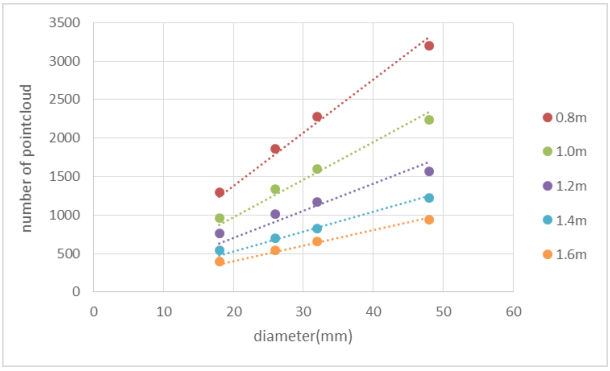

Fig. 3. Diameter of cylinder vs. number of points.

IV. The Estimation of Cylinder Diameter

A. A method using 3D point cloud

The number of 3D points measured from cylinder surface depends on both the measurement area on the cylinder and the distance between a sensor and the cylinder. When the distance to a cylinder is a constant, there is a proportional relationships between the number of points and the measurement area on the cylinder. On the other hand, it is not true that the number of measurement points always the same even when measures the same surface. For instance, the dense of points changes depending on distance to the cylinder. However, it is expected that there is a feasible law that enables to approximately represent their relationship.

Along to such an assumption, we estimate the cylinder diameter by the number of measurement points. The procedure is as follows. First, we specify one image pixel on the area of cylinder as a representative point. Here, we assume that the vector directing from the focal point of a sensor to the representative point intersects with the center core of the cylinder. Next, we calculate 3D coordinates of the representative point using its 2D coordinates and the depth value, and then count the number of points inside the search space with spherical region that centers the representative point.

Here we explains a reason to consider that there is a proportional relationship between cylinder diameter and number of points. A cylinder region inside the spherical space for search can be depicted as a blue rectangular region shown in Fig. 2. Let $d_{cylinder}$ be the cylinder diameter and d_{sphere} be the sphere diameter. We can calculate the long axis length h of the region by the following equation:

$$h = d_{sphere}\sqrt{1 - \frac{d_{cylinder}^2}{d_{sphere}^2}}. \quad (1)$$

When assuming that the cylinder diameter is sufficiently smaller than the sphere diameter, h is approximately equal to d_{sphere}. Thus, the surface area of the cylinder can be calculated by the constant d_{sphere} times the length of radial direction. Furthermore, assuming that the surface area and the density of measurement points are in a proportional relationship, the following equation hold with $d_{cylinder}$ as a variable:

$$n = a \times d_{cylinder}, \quad (2)$$

where n is the number of points and a is a proportionality factor between n and the cylinder diameter.

The following proof experiment was conducted to show the above assumption. Four cylinder objects made of vinyl chloride were prepared. Their diameters were 18, 26, 32, 48 mm, respectively. As 3D range image sensor, Xtion Pro Live made by ASUS Inc. was used. The distances between the sensor and a measurement object were set 0.8 m to 1.6 m with 0.2 m interval. The diameter of spherical search space was set to 160 mm. There were two reasons for determining the diameter value. First, the value is prefer to set relatively larger than the thickest cylinder diameter (48 mm). We confirmed that 160 mm diameter provides practically good results. Second, if we set the sphere space with too large diameter, it prevents to detect cylinders with short length. Note that the search range setting described above is effective only when a cylinder is isolated, such as a ladder or handrail. That is, the setting might not work when there are multiple objects in proximity. If we aim to apply the proposed method in such a situation, we need to specify the target area by applying another filter. This is mentioned in the last subsection of Experiments section.

In Fig. 3, one point shows an average of 10 times estimation results. Horizontal axis indicates number of points and perpendicular axis indicates cylinder diameter. This graph shows that linear approximation works well.

Next, we discuss the relationship between cylinder diameter and the distance from the sensor to the cylinder. In Fig. 3, inclination of the lines differs from the distance and there might be a regularity here. Figure 4 shows a graph about a relationship between the inclination value and the distance. As shown in this graph, a quadratic function is well fitted. Therefore, by preparing an approximate expression using a quadratic function, it is possible to estimate the number of

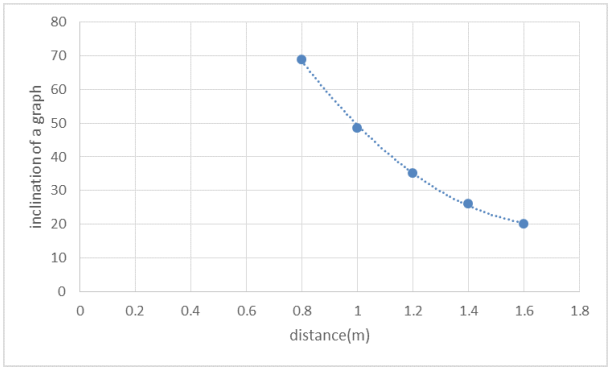

Fig. 4. Distance from the sensor vs. inclination of line

points even when a cylinder is placed at a distance that has not been measured in advance. Using that, we can estimate a cylinder diameter.

B. A method using image edges

It is possible to detect image edges from RGB images. We take an approach to specify edge segments observed from the outline of a cylinder. The cylinder diameter is estimated using the distance between two opposite edges on the outline.

The procedure is as follows. First, as the same as described in the previous subsection, we set spherical search space centering a representative point, and select pixels inside the space. Then, we calculate the long axis of an approximated ellipse obtained by principle component analysis (PCA) to the coordinates of the pixels. Meanwhile, we apply probabilistic Hough transform to extract line segments and then calculate linear equation. By comparing their inclination values with that values of the long axis of the ellipse, we finally obtain line segments which is parallel to the long axis of the ellipse.

As the result of the above processing, it is desirable that one line segment is extracted in each of the right-hand direction and the left-hand direction from the center axis of the cylinder. However, unnecessary edges might remain or a single edge might be cut off due to lighting condition etc. To select correct line segments in such a situation, we take the following procedure. First, the representative point and the cylinder diameter determined at depth image processing is referred, and then the representative point is moved by the amount of the cylinder radius toward the center of the cylinder. In the remaining of this paper, the point obtained in this way is called the cylinder center point.

Next, we select line segments whose distance from the cylinder center point is less than a predefined threshold, which is a value adding a predetermined value to the cylinder radius. Then, we calculate the line equation of each segment, and evaluate its plausibility by counting edgels (pixels constituting edge segments) on the line. Then we determine an edge with the largest number of edgels for both sides of the cylinder.

In the processing described the above, we calculate a cylinder center point using the diameter value obtained from the number of points. Therefore it might be influenced the error arising the former process. However, even in the 3D range image sensor (Xtion PRO Live) mentioned the above, there was almost no influence. For instance, even if 2 mm error occurred in the estimation of cylinder diameter when the cylinder is placed on 0.8 m distant from the sensor, the error rate is 0.25 % because of 2/800. This value is sufficient small. Therefore we assume that two methods describes in the previous and this subsection are independent.

C. Fusion of estimation results

Two results obtained by the above procedures, we calculate the final result. The calculation fomula is as follows:

$$d = \frac{\sigma_{edge}^2}{\sigma_{edge}^2 + \sigma_{point}^2}\mu_{point} + \frac{\sigma_{point}^2}{\sigma_{edge}^2 + \sigma_{point}^2}\mu_{edge}, \quad (3)$$

where d denotes the final estimation result of cylinder diameter. μ_{point} and σ_{point} denote the average and the standard deviation of the diameter estimated using number of 3D points, respectively.

μ_{point} and σ_{point} are calculated from several estimated results. The reason is that in situations where the proposed method should be used, actions such as approaching a target cylinder are often included. In other words, after detecting the cylinder, as it is possible to measure the cylinder multiple times while approaching it, we use the above formula to obtain the final result.

V. Experiments

A. The experimental method

Xtion PRO Live made by ASUS Inc. was used. This range image sensor provides a color image and a depth image sized 640 × 480 pixels with 30 Hz. Measurement targets were four cylinder pipes made of vinyl chloride whose diameters were 18, 26, 32, 48 mm, respectively. First, in order to describe the approximate relationship as shown in Figs. 3 and 4, each cylinder was placed at a distance of 0.8 to 1.6 m from the sensor at intervals of 0.2 m. In each situation, the cylinder was measured as RGB images and depth images. Using them, the coefficients of straight lines and curves were calculated. Figure 5 shows some examples of color images.

Next, each cylinder was placed at a distance of 0.9 m to 1.5 m from the sensor at intervals of 0.2 m. The reason is to show the effectiveness of using function approximation clearly by using different distance conditions from the above. In the cylinder diameter estimation process, the total number of data used to calculate each average and standard deviation was set to 5. Meanwhile, in the process of setting spherical search space, image coordinates of a representative point was manually given by an operator. This is a way based on the premise that human operators investigate the cylinder parameters while they use remote control robots mounting cameras.

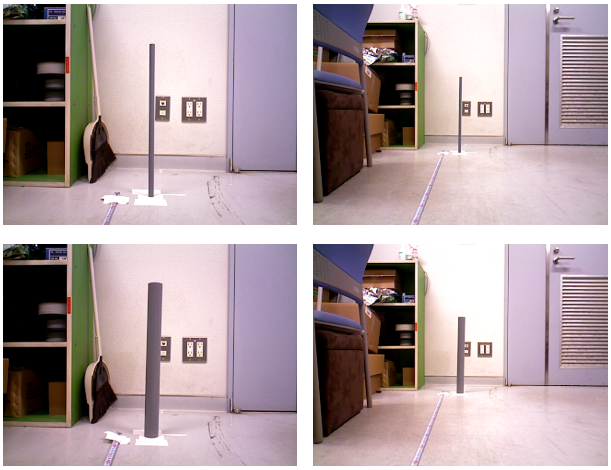

Fig. 5. Examples of sensor data. Top panels show a cylinder with 18 mm diameter. Left photo was captured from 800 mm away, and right photo is captured from 1600 mm away. Bottom panels show a cylinder with 48 mm diameter.

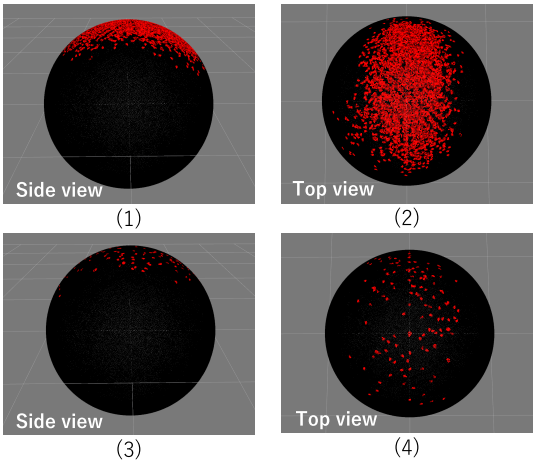

Fig. 6. Gaussian spheres for normal vectors. Top two panels: A result from measurement data obtained by observing a cylinder with a diameter of 48 mm from a distance of 1100 mm, bottom two panels: a result of a cylinder with a diameter of 24 mm from a distance of 1500 mm. In both cases, it is difficult to estimate the direction of cylinder accurately.

B. Applicability of existing methods

The 3D range image sensor used in the experiment was suitable for equipping mobile robots because it is reasonable price and light weight. On the other hand, measurement accuracy was lower than 3D digitizer which is used for product inspection. The data generally holds several to tens mm positional error. For this reason, cylinder detection should be a method that robust to such distance errors.

Using normal information is one major approach for cylinder detection. Methods proposed by Schnabel et al. [9], Trung [14], and Figueiredo et al. [11] are representative work belonging that. Their methods first calculate normal vectors for every 3D points, generate Gaussian sphere, and then estimate the inclination angle of the cylinder part. Next, it estimate the diameter by another method, e.g. Hough transformation. In the former process, thin ring reveals on the Gaussian sphere if measurement data is accurate and then a vector perpendicular from the normal vectors can be calculated correctly. That is, it is important to be able to calculate normal vectors accurately.

Figure 6 shows Gaussian spheres generated from point cloud obtained in this experiment. Upper panels show a result when the cylinder is thick (48 mm) and the distance to the sensor is short (1100 mm), whereas bottom panels show a result when the cylinder is thin (24 mm) and the distance to the sensor is long (1500 mm). The calculation procedure of normal vector was as follows. For every pixels belonging to a cylinder part, pixels whose Manhattan distance from an anchor pixel is two or lower are collected. Then, principle component analysis is applied to the pixels and then normal vector is obtained. After that, a smoothing by averaging neighboring normal vectors is applied. This procedure enables to reduce the error of depth value. However, even if such a procedure, the normal vectors are largely distributed on the Gaussian sphere comparing with the results introduced in Schnabel et al. [4]. This result tells us that it is difficult to apply the approach using normal information for our experiments.

C. Experimental results

Ten measurements were taken for each cylinder and measurement distance, and the average and standard deviation were calculated. Table I shows the results of estimation using the proposed method. For comparison, Table II shows the results when using the functions of Point Cloud Library (PCL) that has a wide track record of use in object grasping by robots, and so on [17][18][19]. In PCL, the number of sampling was 10,000 times, the weight for the surface normal was 0.1, and the distance threshold to the cylinder model was 50 mm. These settings were the result of adjusting as much as possible to obtain the best value.

The computer used in the experiment had a CPU of Xeon 3.5 GHz and a memory with 32 GB. The processing time for PCL was as follows. When the data size of the point cloud was the largest (the distance between the sensor and the cylinder was the nearest, 0.8 m), the average processing times for 10 measurement data were 0.910 sec for cylinder diameter 18 mm, 0.977 sec for 26 mm, 1.035 sec for 32 mm, and 1.544 sec for 46 mm. On the other hand, in the proposed method, processing times were as follows: 1.138 sec for 18 mm, 1.174 sec for 26 mm, 1.104 sec for 32 mm, and 1.198 sec for 48 mm. From the above, although the processing time of the proposed method is slightly longer, it has hardly changed.

D. Discussion

Comparing Table I and Table II, the results of the proposed method showed that the average error was within 2mm in most cases, and the cylinder diameter could be estimated with better accuracy than PCL. In addition, since the standard deviation value was small, it was found that there was little variation in the estimated cylinder diameter value. On the

TABLE I

RESULTS OF THE PROPOSED METHOD. THE UNIT OF ALL NUMERICAL VALUES IS [MM].

18.0 mm Diameter				
Distance	900	1100	1300	1500
Ave.	17.99	18.90	20.77	21.02
Std.	0.778	0.326	0.338	1.012
26.0 mm Diameter				
Distance	900	1100	1300	1500
Ave.	26.86	27.63	27.61	27.86
Std.	0.773	0.686	1.098	0.469
32.0 mm Diameter				
Distance	900	1100	1300	1500
Ave.	30.31	32.50	32.83	33.89
Std.	0.004	0.190	0.036	0.604
48.0 mm Diameter				
Distance	900	1100	1300	1500
Ave.	47.10	47.54	46.89	47.28
Std.	0.338	0.407	0.323	0.204

TABLE II

RESULTS OF THE METHOD IN PCL

18.0 mm Diameter				
Distance	900	1100	1300	1500
Ave.	16.08	15.97	16.88	18.99
Std.	3.471	0.806	1.037	2.974
26.0 mm Diameter				
Distance	900	1100	1300	1500
Ave.	28.08	25.36	27.17	24.38
Std.	2.813	1.504	3.447	3.877
32.0 mm Diameter				
Distance	900	1100	1300	1500
Ave.	35.15	31.91	28.01	28.76
Std.	3.495	6.482	4.325	4.464
48.0 mm Diameter				
Distance	900	1100	1300	1500
Ave.	55.90	52.62	51.89	42.68
Std.	3.309	6.336	7.270	3.652

other hand, the reason why the standard deviation obtained by the cylinder fitting on PCL was large might be that the robust estimation by RANSAC is used in deriving the cylinder parameters.

Figure 7 and 8 shows the graph of weight values indicated at Eq. (5). In both cases, cylinder diameter was 18 mm. Meanwhile the distance from the sensor was 0.8 m in Fig. 7, and 1.5 m in Fig. 8. At a distance of 0.8 m, the repeatability of the depth value was about 5 mm, and at a distance of 1.5 m, it was about 12 mm.

Comparing the two, the former has a higher priority for the result using point cloud, but there is not much difference. On the other hand, Fig. 9 is a result by image edge was also considered. This was because the depth measurement failed at fourth frame. In such a case, the variance of the estimation result using number of points becomes large, so the priority of the edge-based method becomes high. As a result, the diameter could not be estimated without significant errors.

In the evaluation experiment described the above and the experiment using an actual robot shown below, a vertical or horizontal cylinder was targeted. In both cases, the same parameters as those shown in Figs. 3 and 4 were used. This is because the density of the points that can be measured by the

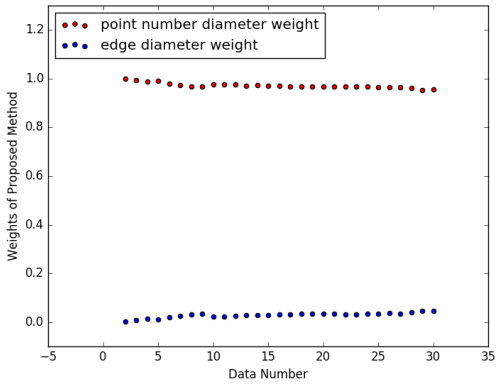

Fig. 7. Weight values on 18 mm cylinder diameter and 0.8 m distance from the sensor.

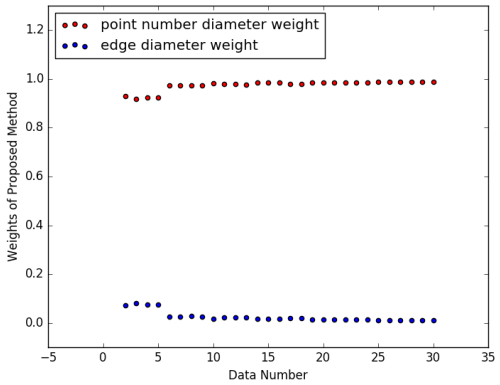

Fig. 8. Weight values on 18 mm cylinder diameter and 1.5 m distance from the sensor.

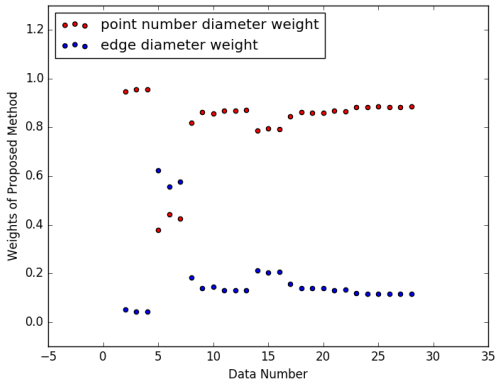

Fig. 9. Weight values on 18 mm cylinder diameter and 1.5 m distance from the sensor, in the case that the depth measurement failed once every 15 frames.

3D range image sensor used this time could be regarded as the same in the vertical and horizontal directions. However, if we must estimate the diameter of a cylinder installed with a certain inclination, the density of points measured on the

surface of the cylinder will be slightly lower. Therefore it is desirable to adjust the parameter of the number of points accordingly. Since the change in density can be calculated from the inclination angle, we can adjust the parameter accordingly after the inclination angle of the cylinder is calculated.

E. Pole grasping by an actual robot

An experimental robot was structured that mounts a 6-DoFs serial link manipulator on a power-wheeled steering mobile platform. The mobile platform was iCart-mini [20] produced by T-frog project and the manipulator was Manipulator-H [21] made by ROBOTIS Inc. ROS was mainly used to implement the software of the robot system and OpenCV 2.4 was especially used to implement the proposed method. A ladder was simulated by combining vinyl chloride pipes as an object to be detected and grasped.

A claw type end-effector sized 100 mm length and 57 mm width was attached to the manipulator. The purpose of the experiment is to hook the ladder by the claw. The initial position of the experimental robot was 1.0 m distant from the ladder. In laterally, it was randomly set within 0.2 m from the front.

In this experiment, the detection of cylinder part to be grasped was automated. The procedure is as follows. First, a depth image is divided into 48 $\times$ 32 grids, and the pixel with the smallest depth value is identified in each grid. Then, pixels having close depth value to the smallest are collected at each grid. Next, the principal component analysis based on the 3D coordinates of those pixels is applied, and grids are retained only when the principal component vector is oriented horizontally. The reason for doing this is that the ladder bars are generally mounted parallel to the ground. After that, clustering is performed on the remaining 3D point cloud. Then, based on the center point of each cluster, the cylinder diameter is estimated using the number of points. Finally, the cluster with the highest number of points is identified as the object to be grasped.

In the above processing, there is a possibility that 3D points measured from parts other than horizontal cylinders is mixed at the clustering stage. However, since the spherical search space is set around the center point, only the points within the range are used for the estimation of cylinder diameter. At least in this experiment, there was no problem related to such unnecessary points. Based on the above results, the robot moved and tried to hook the ladder onto the crosspiece. As shown in Fig. 10, the hooking task was achieved.

The experiment mentioned the above shows an implementation example along the purpose of this study. However, the implementation might be not widely applicable because it is assumed that cylindrical parts exist sparsely. From the viewpoint to estimate the state of cylindrical objects, it is desirable to extend the method so that it can be applied even in more complex environments. Therefore, let us consider an approach that applies existing methods to the detection of cylinder candidates. However, as previously introduced,

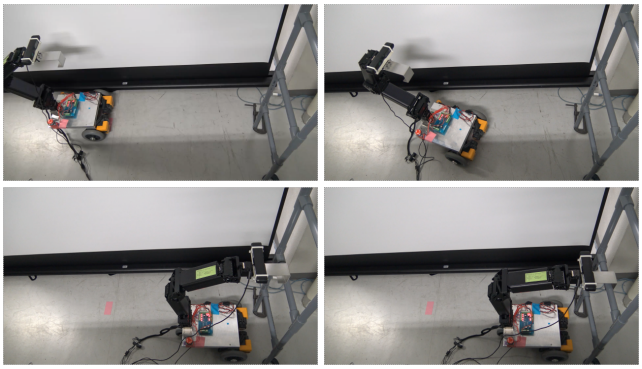

Fig. 10. Snapshots of an experiment using an actual robot

general-purpose 3D range image sensors have insufficient data measurement accuracy to apply the method using normal information. On the other hand, there are methods that use a detector that responds strongly to the partial region derived from the cylinder. Mitash et al. [15] adopted a method of outputting a candidate area of specific objects as a heat map from a cluttered environment. It is a preprocessing for applying Super 4PCS which is a method for collating two point clouds. In the cylinder detection problem, it will be possible to specify the cylindrical area necessary for diameter estimation by determining the seed point by the same way and then applying segmentation by region growing method [16] etc.

VI. Conclusion

In this paper, we proposed a novel method for obtaining the cylinder diameter. We formulated the relationship between cylinder diameter and the number of 3D point cloud measured from the cylinder. Using the combination with image edges, we confirmed that the proposed method enables to obtain cylinder diameter about 2 mm or less error. Moreover, as an example of the search activity at disaster environments, we conducted an experiment on grasping a ladder by a remote control robot.

Future work includes the improvement of estimation accuracy. One of the ways is to device a relational expression that takes into account the measurement method. As mentioned in Section V, another useful extension is to combine a preprocessing for obtaining candidate regions of cylindrical parts with the proposed method. It is also expected that the formulation of the proposed method is extended to cope with cylinders existing at various orientations. To extend the estimation targets is also important. If we can deal with objects such as elliptical cylinder, prisms, and torus, the number of objects that the robot can grasp will increase. Moreover, it is desirable to assist remote controlled work by robots using cylinder information.

References

[1] Tadokoro, Satoshi (Ed.), “Disaster Robotics -Results from the ImPACT Tough Robotics Challenge-,” Springer, ISBN 978-3-030-05321-5, 2019.

[2] T. Matsuzawa et al. “End-effector with a Hook and Two Fingers for the Locomotion and Simple Work of a Four-limbed Robot,” in Proc. of the 2018 IEEE/RSJ International Conference on Intelligent Robots and Systems, pp. 2727-2732, 2018.
[3] Point Cloud Library, http://pointclouds.org/
[4] R. Schnabel, R. Wahl and R. Klein, “Efficient RANSAC for Point-Cloud Shape Detection,” Computer Graphics Forum, vol.26, no.2, pp.214 - 226, 2007.
[5] M. A. Fischler and R. C. Bolles, “Random Sample Consensus: A Paradigm for Model Fitting with Applications to Image Analysis and Automated Cartography” Comm. ACM. 24 (6): 381395, 1981.
[6] L. C. Goron, Z. Marton, G. Lazea, M. Beetz, “Robustly Segmenting Cylindrical and Box-like Objects in Cluttered Scenes using Depth Cameras,” 7th German Conference on Robotics, Munich, Germany, pp. 1-6, 2012.
[7] S. Kim and M. Likhachev, “Planning for grasp selection of partially occluded objects,” in Proc. of IEEE Int’l Conf. on Robotics and Automation, pp. 3971-3978, 2016.
[8] G. Vosselman, B. Gorte, G. Sithole, T. Rabbani, “Recognising structure in laser scanner point clouds,” International Archives of Photogrammetry, Remote Sensing and Spatial Information Sciences 46, 8/W2, pp. 3338, 2004.
[9] T. Rabbani and F. Van Den Heuvel, “Efficient hough transform for automatic detection of cylinders in point clouds,” ISPRS WG III/3, III/4, vol. 3, pp. 6065, 2005.
[10] K. Harada, K. Nagata, T. Tsuji, N. Yamanobe, A. Nakamura, Y. Kawai, “Probabilistic approach for object bin picking approximated by cylinders,” in IEEE International Conference on Robotics and Automation, pp. 37423747, 2013.
[11] R. Figueiredo, P. Moreno and A. Bernardino, “Robust cylinder detection and pose estimation using 3D point cloud information,” in Proc. of IEEE Int’l Conf. on ICARSC, pp.234 - 239, 2017.
[12] J. F. Lalonde, N. Vandapel and M. Hebert, “Automatic three dimensional point cloud processing for forest inventory,” CMU-RI-TR-06-21, Robotics Inst., CMU, 2006.
[13] Eiichi Horiuchi, “Automatic Detection of Tree-trunks by Fitting Cylinders to 3D Point Clouds,” Journal of Robotics Society Japan, Vol.31, No.6, pp. 605 - 613, 2013. (in Japanese)
[14] T. Tran, V. Cao, D. Laurendeau: “Extraction of cylinders and estimation of their parameters from point clouds,” Computer & Graphcis, Vol. 46, pp. 345 – 357, 2014.
[15] C. Mitash, A. Boularias, K. E. Bekris: “Robust 6D Object Pose Estimation with Stochastic Congruent Sets,” in the proc. of the British Machine Vision Conference (BMVC), 2018.
[16] K. Yamazaki, K. Sogen, T. Yamamoto, M. Inaba: “Feasibility Study of Textureless Object Detection and Pose Estimation Based on a Model with 3D Edgels and Surfaces,” Journal of Behavioral Robotics, Vol. 6, Issue 1, pp. 191 204, 2015.
[17] R. B. Rusu, N. Blodow, Z. C. Marton, and M. Beetz: “Close-range Scene Segmentation and Reconstruction of 3D Point Cloud Maps for Mobile Manipulation in Human Environments,” in Proc. of IEEE/RSJ Int’l Conf. on Intelligent Robots and Systems, 2009.
[18] A. ŭckermann, R. Haschke and H. Ritter “Real-time 3D segmentation of cluttered scenes for robot grasping,” in Proc. of 12th IEEE-RAS Int’l Conf. on Humanoid Robots, pp. 198-203, 2012.
[19] Sung-Kyun Kim and M. Likhachev: “Planning for grasp selection of partially occluded objects,” in Proc. of IEEE Int’l Conf. on Robotics and Automation, pp. 3971-3978, 2016.
[20] http://t-frog.com/products/icart_mini/
[21] http://www.robotis.us/robotis-manipulator-h/